5. L. Eits, Principles of Fluidization Mechanics with Applications [Russian translation], Moscow (1986).
6. I. P. Mukhlenov, B. S. Sazhin, V. F. Frolov, et al., Calculations of Boiling-Bed Equipment (Handbook) [in Russian], Leningrad (1986).
7. D. Himmelblau, Applied Nonlinear Programming [Russian translation], Moscow (1975).
8. A. A. Samarskii, Theory of Difference Schemes [in Russian], Moscow (1977).
9. V. A. Novikov, Zh. Vychisl. Mat. Mat., No. 3, 385-390 (1987).

COLLECTOR HEAT EXCHANGER WITH VARIABLE COOLANT PROPERTIES

V. A. Babenko

UDC 536.48

A mathematical model of the cooling of a porous heat-liberating tube between a coaxial tube and a channel of annular cross section is proposed and realized.

The delivery of heat carrier through the lateral wall of one channel and its collection in another coaxial channel is a widely used method in heat exchangers, chemical reactors, and power plants [1, 2]. On cooling extended porous elements, the use of a transverse filtration scheme ensures multiple reduction in hydraulic expenditures in comparison with the longitudinal scheme.

One possible deficiency of the transverse-filtration scheme (the so-called collector scheme) is nonuniformity of filtration over the length of the apparatus, which reduces its effectiveness and may facilitate the development of an emergency. Reducing the nonuniformity entails rational choice of the cross sections of the delivery and collection channels, as well as the wall porosity.

The method of heat-exchanger calculation is to solve the parabolic momentum and energy equations in the channels and in the porous wall, matching the solutions at the boundaries of the calculation regions in accordance with external and internal boundary conditions.

Four regions of radius variation are isolated (Fig. 1) in the cylindrical coordinate system (r, x): a) the central tube, $r \in (0, a)$; b) the internal region of the annular channel, $r \in (b, f)$; c) the outer region of the annular channel, $r \in (f, c)$; d) the porous wall, where r = f, the radius of maximum velocity in the annular channel.

The equations of mass, momentum, and energy balance are now written in one of the flow regions a, b, or c in the channels

$$\frac{\partial (r\rho u)}{\partial x} + \frac{\partial (r\rho v)}{\partial r} = 0, \tag{1}$$

$$\rho u \frac{\partial u}{\partial x} + \rho v \frac{\partial u}{\partial r} = -\frac{dP}{dx} + \frac{1}{r}\frac{\partial (r\tau)}{\partial y}, \tag{2}$$

$$\rho u \frac{\partial h}{\partial x} + \rho v \frac{\partial h}{\partial r} = \frac{1}{r}\frac{\partial}{\partial y}(rq), \tag{3}$$

where $y = |r - r_w|$ is the distance from the corresponding wall; the shear stress τ and heat-flux density q are defined as follows

$$\tau = \rho \nu \nu_{eff} \frac{\partial u}{\partial y}, \tag{4}$$

A. V. Lykov Institute of Heat and Mass Transfer, Academy of Sciences of the Belorussian SSR, Minsk. Translated from Inzhenerno-Fizicheskii Zhurnal, Vol. 59, No. 1, pp. 131-140, July, 1990. Original article submitted October 21, 1988.

 0022-0841/90/5901-0928$12.50

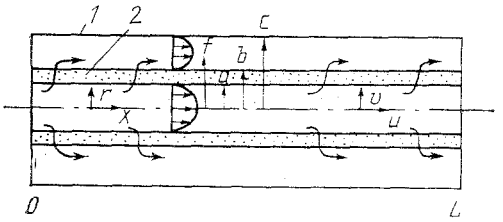

Fig. 1. Diagram of heat exchanger; 1) casing; 2) heat-liberating porous tube; a, b, c, wall radii; f, radius of maximum velocity in annular channel.

$$q = \rho\nu \frac{\mathrm{Pr}_m}{\mathrm{Pr}} \frac{\partial h}{\partial y}, \tag{5}$$

where

$$\nu_{\mathrm{eff}} = 1 + \frac{\nu_t}{\nu}, \quad \mathrm{Pr}_m = \left(1 + \frac{\nu_t}{\nu}\frac{\mathrm{Pr}}{\mathrm{Pr}_t}\right) \Big/ \nu_{\mathrm{eff}}.$$

Suppose that the coolant motion in the porous wall occurs in a radial direction and conforms to Darcy's law. Local temperature equality of the frame of the porous body and the coolant within the wall is assumed. The basis for these and other assumptions in the formulation of the problem was considered in [3].

The equations of mass, momentum, and energy balance in the porous wall take the form

$$\frac{\partial (r\rho v)}{\partial r} = 0, \tag{6}$$

$$\rho v = -\frac{K}{\nu}\frac{\partial P}{\partial r}, \tag{7}$$

$$\rho v \frac{\partial h}{\partial r} = \dot{q}_v + \frac{1}{r}\frac{\partial}{\partial r}\left(r\frac{\Lambda}{c_p}\frac{\partial h}{\partial r}\right) + \frac{\partial}{\partial x}\left(\frac{\Lambda}{c_p}\frac{\partial h}{\partial x}\right). \tag{8}$$

For the axial velocity component, the boundary conditions of adhesion at the impermeable and permeable walls of the channels are assumed. At the external boundary r = c, the heat flux q_{wc} = const is specified; at the central axis, the symmetry conditions $\partial h/\partial r = 0$, $\partial u/\partial r = 0$, v = 0 are specified. At the internal boundaries r = a and r = b, continuity conditions are assumed for the pressure, the radial velocity component v and the enthalpy. The velocity in the porous medium is understood to be the mean velocity through unit cross section. The boundary conditions for matching of the heat flux at r = a and r = b take account of the possibility that there are surface heat sources at these boundaries: $[q_{wi}] + \dot{q}_{wi}/2\pi r_{wi} = 0$, i = a, b, where $[q_{wi}]$ is the jump in q_w at the boundary $r = r_{wi}$; $\dot{q}_{wi}$ is the power of the surface source.

Converting Eqs. (1)-(8) to dimensionless form, all the linear dimensions are divided by $L = \sqrt{(S_\Sigma/2\pi)}$; the enthalpy by the enthalpy at the input h_0; the velocities u and v by $u_0 = G_\Sigma/\rho_0 S_\Sigma$; P and τ by ρu_0^2; q by $\rho_0 u_0 h_0$; $\dot{q}_V$ by $\rho_0 u_0 h_0/L$; $\dot{q}_{(w,v,d)}$ by $G_\Sigma h_0/L$; and S by S_Σ. The thermophysical properties are referred to the corresponding quantities in the input conditions. The dimensionless quantities will be denoted by the same symbols. In the cases where it is necessary to emphasize that dimensional quantities are meant, it is conventional to add an asterisk.

As a result of integrating the initial Eqs. (1)-(3) and (6)-(8) over the cross section of the regions a, b, c, and d, a system of ordinary differential equations in terms of the variable is obtained

$$(\omega_a)'_x = -j, \tag{9}$$

$$-S_a (P_a)'_x = a\tau_{wa} + \beta_a \delta_a \left(-\frac{2j}{\omega_a} - (\bar{\rho}_a)'_{lx}\right), \tag{10}$$

$$-S_{\kappa}(P_{\kappa})'_x = b\tau_{wb} + c\tau_{wc} + \beta_{\kappa}\delta_{\kappa}\left(\frac{2j}{\omega_{\kappa}} - (\bar{\rho}_{\kappa})'_{lx}\right), \tag{11}$$

$$\omega_a(\bar{h}_a)'_x = -aq_{wa} - j(h_{wa} - \bar{h}_a), \tag{12}$$

$$\omega_b(\bar{h}_b)'_x = -bq_{wb} + fq_{eb} + j(h_{wb} - \bar{h}_b) - j_f(h_{eb} - \bar{h}_b), \tag{13}$$

$$\omega_c(\bar{h}_c)'_x = -cq_{wc} + fq_{ec} + j_f(h_{ec} - \bar{h}_c), \tag{14}$$

$$(Q)'_x = -\dot{q}_d - bq_{wd} - aq_{wa} + j(h_{wb} - h_{wa}), \tag{15}$$

$$S_d(\bar{h}_d)'_x = \mathrm{Pe}_d Q, \tag{16}$$

where $j=\rho_{wa}v_{wa}$ $a=\rho_{wb}v_{wb}$ $b=\rho vr$ is the dimensionless transverse mass flux; $(\bar{\rho})_{\ell x}'$ is the logarithmic derivative of the density $\bar{\rho}$; $\mathrm{Pe_d} = G_{\Sigma}\bar{c}_{pd}/\Lambda_d L 2\pi$ is a dimensionless complex.

Equation (9) is the integral mass-balance equation in the central tube; Eqs. (10) and (11) are the momentum balance equations in the tube and the annular channel; and Eqs. (12)-(15) are the thermal balance equations in regions a, b, c, and d. Equation (16) describes the heat propagation by conduction along the porous wall.

Integration of Eq. (7) over the radius of the porous wall gives a relation between the flow rate j and the pressure difference between the channels $P_a - P_k$

$$j = \frac{\tilde{K}N}{\nu_d}(P_a - P_{\kappa}). \tag{17}$$

The friction at the walls and the coefficients of the momentum flux and the heat fluxes in Eqs. (9)-(16) are determined from the solution of the boundary problems for the radial velocity and enthalpy distributions.

Suppose that the enthalpy field in the porous wall is self-similar with respect to the longitudinal coordinate, i.e., $h = h_1(r)\bar{h}_d(x)$, and that the effective thermal conductivity of the porous wall Λ and the specific heat of the gas at the wall c_p are equal to their mean values over the wall cross section. In this case, variable separation is possible in Eq. (8), which leads to the boundary problem for an ordinary differential equation in terms of the function $h_1(r)$. Solving this problem, the following expression is obtained for the radial enthalpy distribution in the porous wall

$$h - \bar{h}_d = \frac{\mathrm{Pe}_d}{z_1}\left[\frac{-(\Gamma_a+\Gamma_b)r^{\vartheta}}{\vartheta} + (\Gamma_b a^{\vartheta-2} + \Gamma_a b^{\vartheta-2})\left(\frac{2r^2+b^2+a^2}{4}\right) + \right.$$

$$\left. + \frac{(\Gamma_a+\Gamma_b)(b^{\vartheta+2} - a^{\vartheta+2})}{\vartheta(\vartheta+2)S_d}\right],$$

where $\Gamma_a = \frac{b}{a}(aq_{wa} + \dot{q}_{wa})$, $\Gamma_b = \frac{a}{b}(bq_{wb} + \dot{q}_{wb})$, $z_1 = a^{\vartheta-1}b - b^{\vartheta-1}a$, $\vartheta = j\mathrm{Pe}_d$.

The expression for the enthalpy difference across the wall gives the result

$$h_{wb} - h_{wa} = \frac{\mathrm{Pe}_d}{z_1}\left[(\Gamma_b a^{\vartheta-2} + \Gamma_a b^{\vartheta-2})S_d - (\Gamma_a+\Gamma_b)\frac{(b^{\vartheta} - a^{\vartheta})}{\vartheta}\right]. \tag{18}$$

The velocity and enthalpy distribution in regions a, b, and c is now determined. Integrating Eq. (2) with respect to the radius from the wall $r = r_w$ to r gives

$$\int_{r_w}^{r}\frac{\partial}{\partial x}(r\rho u^2)\,dr + r\rho v u = -\frac{dP}{dx}\frac{r^2 - r_w^2}{2} + \mathrm{sgn}(r\tau - r_w\tau_w), \tag{19}$$

where the function sgn takes the values −1, 1, −1, respectively for regions a, b, and c.

Substituting $r\rho v$ from Eq. (1) into Eq. (19) and introducing the following dimensionless coordinates and variables

$$\varepsilon = (r^2 - r_w^2)/(r_e^2 - r_w^2),\ \xi = \frac{r\tau}{\delta},\ p = \frac{SP'_x}{\delta},\ j_w = r_w\rho_w v_w\,\mathrm{sgn},$$

the tangential frictional force in the flux ξ is found in the form

$$\xi = \xi_w + \varepsilon p + \frac{j_w}{\omega}\tilde{u} + \frac{1}{\overline{p}\,\overline{u}^2}\left[\int_0^\varepsilon \frac{\partial(\rho u^2)}{\partial x}\,d\varepsilon - u\int_0^\varepsilon \frac{\partial(\rho u)}{\partial x}\,d\varepsilon\right]. \tag{20}$$

Determining the dimensionless current function U_1 from the relation

$$\frac{\partial U_1}{\partial \varepsilon} = \tilde{\rho}\tilde{u} \tag{21}$$

and integrating Eq. (20) with respect to ε, the result obtained, after appropriate manipulations, is

$$\frac{\partial \xi}{\partial \varepsilon} = p + \frac{j_w}{\omega}\frac{\partial \tilde{u}}{\partial \varepsilon} + \left(\frac{\tilde{\rho}\tilde{u}}{\overline{u}}\right)\frac{\partial}{\partial x}(\overline{u}\tilde{u}) - \frac{\partial \tilde{u}}{\partial \varepsilon}\frac{1}{\omega}\frac{\partial(U_1\omega)}{\partial x}. \tag{22}$$

In dimensionless form, Eq. (4) is as follows

$$\frac{\partial \tilde{u}}{\partial \varepsilon} = F_1\xi, \tag{23}$$

where $F_1 = S\omega N/r^2\mu\nu_{eff}$.

Within the framework of the boundary-layer approximation, the derivative of the pressure with respect to the longitudinal coordinate does not depend on the radius. Therefore

$$\frac{\partial p}{\partial \varepsilon} = 0. \tag{24}$$

Together with the boundary conditions $\varepsilon = 0$: $\tilde{u} = U_1 = 0$; $\varepsilon = 1$: $\varepsilon = 0$, $U_1 = 1$, Eqs. (21)-(24) form the boundary problem for determining the functions ξ, $\tilde{u}$, U_1, p.

The boundary problem for the distribution of the enthalpy over the radius is derived analogously, and therefore is written at once

$$\frac{\partial U_2}{\partial \varepsilon} = \tilde{\rho}\tilde{u}\hat{h}, \tag{25}$$

$$\frac{\partial \zeta}{\partial \varepsilon} = \frac{j_w}{\omega}\frac{\partial \hat{h}}{\partial \varepsilon}\tilde{\rho}\tilde{u}\frac{\partial \hat{h}}{\partial x} - \frac{1}{\omega}\frac{\partial \hat{h}}{\partial \varepsilon}\frac{\partial(\omega U_1)}{\partial x} + \tilde{\rho}\tilde{u}H, \tag{26}$$

$$\frac{\partial \hat{h}}{\partial \varepsilon} = F_2\zeta, \tag{27}$$

$$\frac{\partial H}{\partial \varepsilon} = 0, \tag{28}$$

$$\varepsilon = 0\colon\ \zeta = \zeta_{w\text{M}},\ U_2 = 0;\quad \varepsilon = 1\colon\ \zeta = \zeta_{e\text{M}},\ U_2 = 0,$$

where $F_2 = Pr/Pr_m F_1$, $\hat{h} = h - \overline{h}$, $H = d\overline{h}/dx$.

The boundary problems in Eqs. (21)-(24) and Eqs. (25)-(28) are solved numerically by the matrix-fitting method [3] at each step with respect to the longitudinal coordinate and in each region with respect to ε.

The most expedient algebraic models for calculating the characteristics of turbulent transfer ν_t and Pr_t are the Reichart and Van Driest models [4], since numerous generalizations for complex boundary conditions and nonisothermal flow are known for these models. An expansion of the Reichart model to flow at small Reynolds numbers is used in the calculations [5]. The well-known generalization to flow in an annular channel [6] is applied to the model transformed in this way, together with a transformation [7] to take account of nonisothermal conditions and injection–suction. The latter two effects influence the radial distribution of the tangential friction and heat flux similarly, and may therefore be taken into account in the same way.

The turbulent Prandtl number Pr_t is taken to be $Pr_t = 0.9$.

The interaction between different parts of the algorithm is now described. The boundary problems in Eqs. (21)-(24) and (25)-(28) are solved nuemrically by the matrix-fitting method successively in each layer with respect to x, with iterations for refinement of the

thermophysical properties and velocity profiles. The solutions of the boundary problems in regions a, b, c, d are matched according to the conditions of equal pressure gradients in regions b and c

$$\frac{\delta_b}{S_b} p_b = \frac{\delta_c}{S_c} p_c, \tag{29}$$

continuity of the longitudinal velocity component at point r = f

$$\tilde{u}_{eb} \frac{\delta_b}{\omega_b} = \tilde{u}_{ec} \frac{\delta_c}{\omega_c} \tag{30}$$

and continuity of the enthalpy field.

Closure of the system in Eqs. (9)-(16) requires a method of calculating the position of the velocity maximum in the annular channel, i.e., S_c, the flow rate ω_c, and the rate of overspill from region b into region c, $j_f = (\omega_c)_x'$. To this end, neglecting the derivatives of the momentum-flux coefficients β_b, β_c, the momentum balance equations are written separately for regions b and c

$$\beta_b (\delta_b)_{lx}' - \tilde{u}_{eb} (\omega_b)_{lx}' = - p_b - \tau_{wb} - \frac{j}{\omega_b} \tilde{u}_{eb}, \tag{31}$$

$$\beta_c (\delta_c)_{lx}' - \tilde{u}_{ec} (\omega_c)_{lx}' = - p_c - \tau_{wc} \tag{32}$$

and p_b and p_c are excluded from Eqs. (31) and (32) using the condition in Eq. (29). The result obtained is

$$\begin{aligned} &\frac{\delta_b \beta_b}{S_b} (\delta_b)_{lx}' - \frac{\delta_c \beta_c}{S_c} (\delta_c)_{lx}' - \tilde{u}_{eb} \frac{\delta_b}{S_b} (\omega_b)_{lx}' + \tilde{u}_{ec} \frac{\delta_c}{S_c} (\omega_c)_{lx}' = \\ &= - \tau_{wb} \frac{\delta_b}{S_b} + \tau_{wc} \frac{\delta_c}{S_c} - \frac{j}{\omega_b} \frac{\delta_b}{S_b} \tilde{u}_{eb}. \end{aligned} \tag{33}$$

Differentiating the velocity continuity condition in Eq. (30) and the mass balance equation $\omega_k = \omega_b + \omega_c$ gives the following result after neglecting the small derivatives $(\tilde{u}_{eb})_{\ell x}'$ and $(\tilde{u}_{ec})_{\ell x}'$

$$(\delta_b)_{lx}' - (\omega_b)_{lx}' = (\delta_c)_{lx}' - (\omega_c)_{lx}', \tag{34}$$

$$\omega_{bk} (\omega_b)_{lx}' + \omega_{ck} (\omega_c)_{lx}' = \frac{j}{\omega_k}. \tag{35}$$

One more differential equation is derived by differentiating the balance condition for the cross section $S_k = S_b + S_c$ with respect to x. Taking into account that $\delta_i = \omega i^2 / S_i \bar{\rho}_i$, i = b, c, it follows that

$$S_b (2 (\omega_b)_{lx}' - (\delta_b)_{lx}' - (\bar{\rho}_b)_{lx}') + S_c (2 (\omega_c)_{lx}' - (\delta_c)_{lx}' - (\bar{\rho}_c)_{lx}') = 0. \tag{36}$$

Solution of the system in Eqs. (31)-(36) with respect to $(\omega_c)_{\ell x}'$ and $(\delta_c)_{\ell x}'$ gives

$$\begin{aligned} &(\omega_c)_x' \left[\frac{\delta_b}{\omega_b} \left(\frac{(\tilde{u}_{eb} - \beta_b)}{S_b} + \frac{\beta_b}{\omega_c} \left(\frac{\omega_b}{S_b} - \frac{\omega_k}{S_k} \right) \right) + \right. \\ &\left. + \frac{\delta_c}{\omega_c} \left(\frac{(\tilde{u}_{ec} - \beta_c)}{S_c} + \frac{\beta_c}{\omega_b} \left(\frac{\omega_c}{S_c} - \frac{\omega_k}{S_k} \right) \right) \right] = - \tau_{wb} \frac{\delta_b}{S_b} + \\ &+ \tau_{wc} \frac{\delta_c}{S_c} - \frac{\beta_b \delta_b}{S_b} \frac{j}{\omega_b} + \left(\frac{\beta_b \delta_b}{S_b} - \frac{\beta_c \delta_c}{S_c} \right) \left(S_{bk} (\bar{\rho}_b)_{lx}' + \right. \\ &\left. + S_{ck} (\bar{\rho}_c)_{lx}' - S_{bk} \frac{j}{\omega_b} \right), \\ &(\delta_c)_x' = \delta_c \left[\left(2 - \frac{S_{\ell k}}{\omega_{bk}} \right) (\omega_c)_{lx}' - (S_{bk} (\bar{\rho}_b)_{lx}' + S_{ck} (\bar{\rho}_c)_{lx}') - j/\omega_b \right]. \end{aligned} \tag{37}$$

Regarding Eq. (37) as the basic equation, it is added to the system to be solved in Eqs. (9)-(16). The latter expression for $(\delta_c)_x'$ is auxiliary, and is used in the predictor

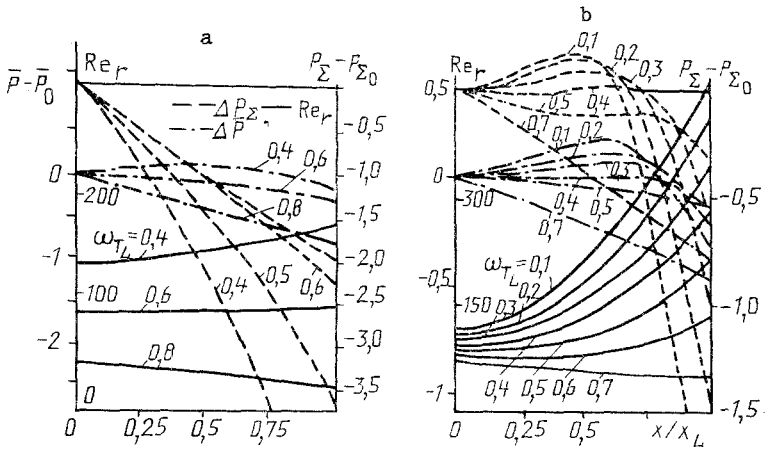

Fig. 2. Variation in pressures $\Delta\bar{P}$, ΔP_Σ and Reynolds number of overflow Re_r over the length: helium coolant, P = 1 atm, $t_{T_0} = t_{k_0} = 6$ K, $\omega_{t_0} = 0.9$, $K = 1\cdot10^{-12}$ m^2 (a), $4\cdot10^{-2}$ m^2 (b), $a = 6$ mm, b = 8.5 mm, c = 12 mm, $x_L = 0.6$ m.

stage of determining S_c in the next layer with respect to x, $S_c = \omega_c^2/\delta_c\bar{\rho}_c$. After solving the boundary problems, the cross sections of regions b and c are refined from the matching condition for the profiles: $\tilde{u}_{eb}\omega_b/S_b\bar{\rho}_b = \bar{u}_{ec}\omega_c/S_c\bar{\rho}_c$.

Obvious relations for matching the enthalpy field are

$$\hat{h}_{wa} - \hat{h}_{wb} + (h_{wb} - h_{wa}) = \bar{h}_b - h_a, \tag{38}$$

$$\hat{h}_{eb} - \hat{h}_{ec} = \bar{h}_c - \bar{h}_b, \tag{39}$$

$$\hat{h}_{wa} - (h_{wa} - \bar{h}_d) = \bar{h}_d - \bar{h}_a \tag{40}$$

and Newtonian linearization of the dependences $\hat{h}_w = \hat{h}_w(\zeta_w, \zeta_e)$, $\hat{h}_e = \hat{h}_e(\zeta_w, \zeta_e)$ is expedient

$$\hat{h}_w = \hat{h}_{wM} + \left(\frac{\partial\hat{h}_w}{\partial\zeta_{wM}}\right)(\zeta_w - \zeta_{wM}) + \left(\frac{\partial\hat{h}_w}{\partial\zeta_{eM}}\right)(\zeta_e - \zeta_{eM}), \tag{41}$$

$$\hat{h}_e = \hat{h}_{eM} + \left(\frac{\partial\hat{h}_e}{\partial\zeta_{wM}}\right)(\zeta_w - \zeta_{wM}) + \left(\frac{\partial\hat{h}_e}{\partial\zeta_{eM}}\right)(\zeta_e - \zeta_{eM}). \tag{42}$$

Substituting Eqs. (41) and (42) into Eqs. (38)-(40), a system of three linear algebraic equations for ζ_{wa}, ζ_{wb}, and ζ_{eb} is obtained. It is taken into account here that $\zeta_{ec} = -\omega_b/\omega_c\zeta_{eb}$. To solve these equations, it is necessary to know $\hat{h}$, $\partial\hat{h}/\partial\zeta_w$, $\partial\hat{h}/\partial\zeta_e$ at the ends of a unit interval in ε, i.e., the solution of the boundary problems for $\hat{h}$, $\partial\hat{h}/\partial\zeta_w$, $\partial\hat{h}/\partial\zeta_e$. The grid functions $\partial\hat{h}/\partial\zeta_w$ and $\partial\hat{h}/\partial\zeta_e$ are determined in the same fitting cycle with respect to ε as for $\hat{h}$. The boundary problems for all three functions are similar, which means that the volume of computational work increases only slightly in comparison with the solution of the boundary problem for $\hat{h}$ alone. The boundary problems for $\partial\hat{h}/\partial\zeta_w$ and $\partial\hat{h}/\partial\zeta_e$ may easily be obtained by differentiating Eqs. (25)-(28) with respect to the corresponding parameter.

The algorithm and programs are tested by comparing the calculation results with known literature data for constant coolant properties; the agreement is good, for both the hydrodynamic and thermal quantities.

Analysis of the results on the hydraulic drag and heat-transfer coefficient in the collector heat exchanger are complex in view of the simultaneous action of several factors: the variable (over the length) flow rate in both channels; the presence of input hydrodynamic and thermal sections, the length of which depends on the rate of overflow; the variability of the rate of overflow itself; and the variability of the thermophysical properties. In the present work, the problem of determining the quantitative contribution of each effect is not posed. The heat exchanger is studied as a whole and compared with a prototype: an impermeable tube of the same size introduced into a coaxial frame.

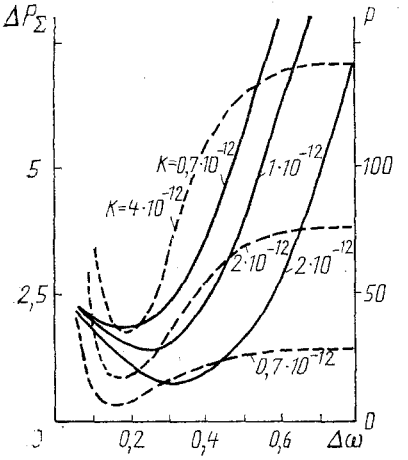

Fig. 3

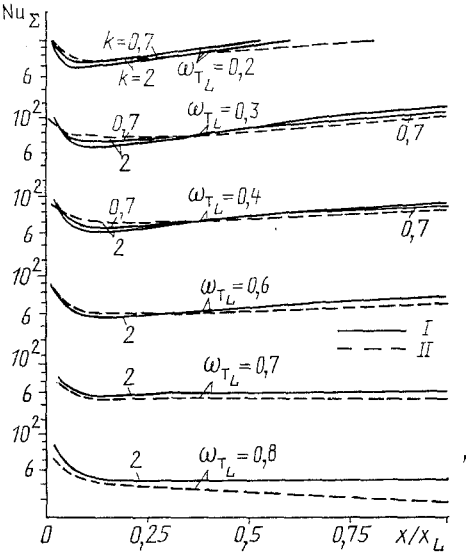

Fig. 4

Fig. 3. Dependence of the pressure drop $\Delta P_\Sigma = P_{\Sigma_0} - P_{\Sigma L}$ and the uniformity of the overflow on the proportion of the overflow; data as in Fig. 2; p, %.

Fig. 4. Comparison of calculation using the data of Fig. 2 with approximation for Nu_Σ: I) calculation (k = 0.7, 2); II) approximation (k = 2).

The variation in the dimensionless overflow rate $Re_r = 2a\rho_\omega a v_\omega a/\mu_0$ depends not only on the geometric configuration and permeability but also on the proportion of overflow from channel to channel (Fig. 2). In the calculations, the boundary condition for the flow rate at the far end is satisfied by the ranging method from the solution of the Cauchy problem, with the ranging parameter $(P_T - P_k)_0$. For the data in Fig. 2, the proportion of the mass flow rate at the input is fixed ($\omega_{T_0} = 0.9$), and the proportion of the flow rate at the output varies. With small suction, the suction rate increases over the length; decrease in ω_{T_L} is accompanied by increase in Re_r at the far end similar to that with a damped far end [1]. With increase in permeability, this increase becomes sharper.

Data on the pressure are analyzed using the mean (over the cross section of both channels) pressure $\overline{P} = St_T P_T + S_k P_k$ and the mean (over the volume) flow rate $P_\Sigma = P_T(\omega_T/\overline{\rho}_T)\rho_\Sigma + P_k(\omega_k/\overline{\rho}_k)\rho_\Sigma$, where $\rho_\Sigma = (\omega_T/\overline{\rho}_T + \omega_k/\rho_k)^{-1}$ is the mean density over the volume. Using the momentum and mechanical-energy balance equations, it may be shown that the drop in $\overline{P}$ gives an idea of the losses due to friction and acceleration of the flux in the channels, while the drop in P_Σ gives an idea of the power consumed in pushing the coolant through the heat exchanger as a whole.

The distribution of the pressures $\overline{P}$, P_Σ (Fig. 2) depends on the parameter characterizing the proportion of overflow ω_{TL} in a complex, nonmonotonic fashion; however, the drop in P_Σ is always greater than the drop in $\overline{P}$. In the initial section, there is restoration of the pressure. With increase in permeability, $Re_{r_0} = f(\omega_{TL})$ is confined within an ever narrower interval. The limiting value $Re_{r_0} \lim_{h\to\infty} Re_{r_0}$ with specified geometry may be obtained from the momentum balance Eqs. (10) and (11) on imposing the condition $P_{T_x}' = P_{k_x}'$.

The dependence of the uniformity of filtration $p = |\Delta j/\overline{j}| = |\Delta j \Delta x/\Delta\omega|$ and the drop in mean-flow-rate pressure P_Σ over the length on the proportion of overflow $\Delta\omega$ is shown in Fig. 3. The curves $\Delta P_\Sigma(\Delta\omega)$ have a minimum; its depth decreases with decrease in K. The existence of a minimum is explained, on the one hand, in that the cross section of the annular channel in this case is large, and it is energetically more favorable to pump a larger part of the flow through the annular channel and, on the other hand, in that this entails pumping the coolant through the porous wall, with consumption of energy. The uniformity basically decreases with decrease in the proportion of overflow. Increase in p at small $\Delta\omega$ is due to the vanishing of the denominator in the expression for p.

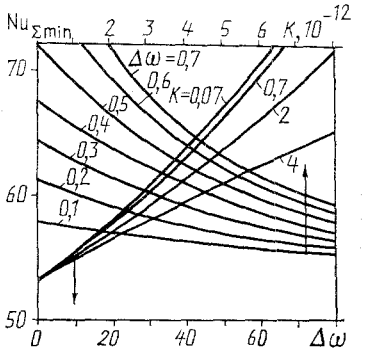

Fig. 5. Dependence of the minimal (over the length) number $Nu_{\Sigma min}$ on the permeability and the proportion of overflow Δw; data as in Fig. 2; K, 10^{-12} m².

Turning to the results for total Nusselt number Nu_Σ for both channels, the expression $Nu_\Sigma = Nu_{\Sigma_0} + Re_r Pr_0/2$ may be used for rough estimation of Nu_Σ, as in the case of isothermal thermophysical properties [8]; the standard Nusselt number Nu_{Σ_0} here is expressed as follows in terms of the Nusselt number in the tube and the annular channel

$$Nu_{\Sigma 0} = (k_{10} + k_{20})/(1 + (\bar{t}_k - \bar{t}_T)\,\bar{\lambda}_d\,(\omega_T k_{20} - \omega_k k_{10})\,\dot{q}_d^{-1}),$$
$$k_{10} = 0.5\,Nu_{T0},\quad k_{20} = 0.5b\,Nu_{k0}/(c-b),$$

while Nu_{T_0} and Nu_{k_0} are calculated from the results of [6, 9, 10], taking account of the presence of the input section and nonisothermality.

The above approximations for Nu_Σ are compared with the results of numerical calculation in Fig. 4. It is significant that, despite the considerable variability in filtration rate (Fig. 2), the variability of the flow rates in the channels, and the variability of the properties (the properties of gaseous helium at input temperature 6 K and atmospheric pressure are used in the calculations), the variation in the Nusselt numbers determining the intensity of cooling of the porous wall as a whole over the length is relatively small.

The minimal (over the length of the cooled section) Nusselt number $Nu_{\Sigma min}$, determining the guaranteed minimum of the cooling intensity, may be of applied interest. As would be expected, this value increases with reduction in permeability (Fig. 5), since the nonuniformity of the overflow decreases, and with increase in the proportion of overflow from the delivery channel to the collection channel on account of the intensification of heat transfer.

NOTATION

x, r, longitudinal and radial coordinates; u, v, longitudinal and radial components of the velocity vector, $\tilde{u} = u/\bar{u}$; P, pressure; t, temperature; h, enthalpy; ρ, density; $\tilde{p} = \rho/\bar{\rho}$; ν, kinematic viscosity; λ, thermal conductivity of coolant; Λ, thermal conductivity of porous wall; c_p, specific heat; $Pr = \nu c_p \rho/\lambda$, laminar Prandtl number; $\dot{q}_v$, volume heat-liberation density in porous body; Q, heat flux along wall; K, permeability, $\tilde{K} = K/L^2 \ln b/a$; S, cross section of region, $S_\Sigma = S_a + S_b + S_c$; $\dot{q}_w$, linear density of heat liberation at surface; $\dot{q}_v = \int_a^b \dot{q}_v r dr$, linear density of volume heat liberation, $\dot{q}_d = \dot{q}_v + \dot{q}_{wa} + \dot{q}_{wb}$; G, flow rate in region, $G_\Sigma = G_a + G_b + G_c$, $\omega = G/G_\Sigma$; $\beta = \overline{\rho u^2}/\bar{\rho}\bar{u}^2$, momentum flux coefficient; $\delta = \omega^2/\bar{S}\rho$, dimensionless momentum flux; $j_f = f\rho_f v_f + u_f(S_c)_{x'}$, dimensionless rate of coolant overflow from region b to region c; $N = Lu_0/\nu_0$; $Nu_T = 2aq_w/\bar{\lambda}_T(t_w - \bar{t}_T)$; $Nu_k = 2(c-b)q_{wb}/\bar{\lambda}_k(t_{wb} - \bar{t}_k)$; $Nu_\Sigma = \dot{q}_d/\lambda_\Sigma = (0.5\,t_{wa} + 0.5\,t_{wb} - t_\Sigma)$; $t_\Sigma = \bar{t}_a\omega_a + \bar{t}_k\omega_k$. Indices: i = a or T, b, c, k, d, in regions with $r \in [0, a]$, [b, f], [f, c], [b, c], [a, b], respectively; w, wall; wi, i-th wall; v, inside wall; 0, at input or in standard conditions; e, external boundary of region (at center of flow); ei, i-th external boundary; t, turbulent value; f, at r = f; L, at the end far from the input.

LITERATURE CITED

1. P. I. Bystrov and V. S. Mikhailov, Hydrodynamics of Collector Heat Exchangers [in Russian], Moscow (1982).
2. I. G. Meerovich and G. F. Muchnik, Hydrodynamics of Collector Systems [in Russian], Moscow (1986).

3. V. A. Babenko, in: Thermal Tubes and Heat Exchangers with Capillary–Porous Elements [in Russian], Minsk (1986), pp. 21-38.
4. B. S. Petukhov, V. D. Vilenskii, and N. V. Medvetskaya, Teplofiz. Vys. Temp., 15, No. 3, 554-565 (1977).
5. V. N. Popov and V. M. Belyaev, Teplofiz. Vys. Temp., 13, No. 2, 370-378 (1975).
6. N. M. Galin and V. M. Esin, Teplofiz. Vys. Temp., 14, No. 5, 991-997 (1976).
7. V. N. Popov, Teplofiz. Vys. Temp., 15, No. 4, 795-801 (1977).
8. V. A. Babenko, in: Heat and Mass Transfer: From Theory to Practice [in Russian], Minsk (1984), pp. 60-65.
9. B. S. Petukhov and L. I. Rozen, Teplofiz. Vys. Temp., 12, No. 3, 565-569 (1974).
10. N. M. Galin and V. M. Esin, Teplofiz. Vys. Temp., 15, No. 6, 1248-1255 (1977).

RADIANT HEAT TRANSFER IN A FURNACE WITH TWO VOLUME ZONES

S. P. Detkov

UDC 536.3

A modification of the model of radiant heat transfer in a furnace for arbitrary transmission of the furnace core is proposed.

1. Introduction

In the mathematical model of [1], a furnace is represented by a cylindrical channel with division along the axis into zones with isothermal volumes in each section. Of course, the model gives significantly overestimated values of the heat transfer or underestimated values of the temperature of the exhaust gases, other conditions being equal. In [2], the model was significantly improved. The volumes in the radial direction are divided into two coaxial layers: the core and a conservative part; the conservative layer (CL) is nonisothermal. Essentially, the core is also nonisothermal, but is characterized by the mean (over the cross section) pyrometric temperature. Some deficiencies of the model may be noted: a) the core is assumed to be optically dense and is replaced by a nontransparent surface with equivalent radiational properties; the model corresponds to a large furnace; b) the spectrum in extreme representations (grey and antigrey) only changes in the CL.

The present model is modified on a new basis. The furnace core may have any transmission characteristics; therefore the model in fact has two volume zones in each cross section of the channel.

The principal underlying this new zonal-calculation approach was outlined in [3, 4]. The volume of the medium is replaced by a surface with equivalent radiative properties. This surface transmits some of the incident flux. Since the volume has a real temperature field, the surface has different local values of the intrinsic-radiation density q_c and other quantities. Therefore, it is divided into zones with mean internal characteristics. In the present work, in contrast to [3-5], the volume is divided into two zones, and the

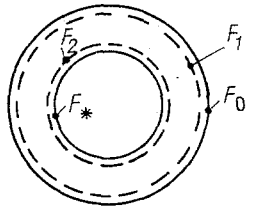

Fig. 1. System of four surfaces: three (F_1, F_2, F_*) represent two volume zones: the core and the conservative layer.

All-Union Scientific-Research Institute of the Power Industry and Nonferrous Metallurgy, Sverdlovsk. Translated from Inzhenerno-Fizcheskii Zhurnal, Vol. 59, No. 1, pp. 141-146, July, 1990. Original article submitted May 3, 1989.

 0022-0841/90/5901-0936$12.50